

Effect of Formulation Variables on Dissolution of Water-Soluble Drug from Polyelectrolyte Complex Beads

e-mail: rvkulkarni75@yahoo.com
ssaleempharm@rediffmail.com

M. A. Saleem^{1,2,*}, Divesh R Kotadia¹, and Raghavendra V. Kulkarni^{3,*}

¹ Department of Pharmaceutics, Luqman College of Pharmacy, Old Jevargi Road, Gulbarga, India

² Department of Biotechnology, Achariya Nagarjuna University, Nagarjuna Nagar, India

³ Department of Pharmaceutical Technology, BLDEA's College of Pharmacy, Bijapur 586103, India

ABSTRACT

This study was planned to develop chitosan-based polyelectrolyte complex (PEC) beads for the prolonged release of the water-soluble drug, verapamil HCl (VPL). The PEC beads were prepared by an ionic gelation method using positively charged chitosan (CH) and negatively charged sodium alginate (ALG), carboxymethylcellulose sodium (CMC), and k-carrageenan (CAR). The surface morphology was investigated by scanning electron microscopy (SEM), and PEC formation was confirmed by differential scanning calorimetry (DSC) and Fourier transform infrared (FTIR) spectroscopy. Gel beads were evaluated for particle size, drug entrapment efficiency, swelling behavior, and in vitro release. The SEM study confirmed that spherical or disc-shaped beads were formed by changing the counterion and pH of the coagulation medium. DSC and FTIR spectroscopy confirmed the PEC formation. The mean particle size was 556–896 μm , and drug entrapment efficiency was more than 80%. The beads showed pH-sensitive swelling with less swelling in hydrochloric acid buffer (pH 1.2) and more swelling in phosphate buffer (pH 7.4). The in vitro release of VPL was very slow in HCl buffer as compared with phosphate buffer. The concentration of chitosan, anionic polymers, and the pH of the coagulation medium significantly affected the size, entrapment efficacy, swelling, and release pattern of PEC beads.

INTRODUCTION

Polycationic chitosan (CH) is prepared through deacetylation of chitin. Chitosan is an important biopolymer having wide pharmaceutical application (1). Chitosan polyelectrolyte complexes (PEC) are ideal substitutes for covalently cross-linked hydrogels. The formation of a PEC requires only polycationic and polyanionic polymers without catalysts or initiators, and the reaction is generally performed in aqueous solution, which is the main advantage over covalently cross-linked polymeric networks. Therefore PEC offers biocompatibility and avoids the purification step to minimize the toxicity associated with the unreacted covalent cross-linking agents before administration (2–6). The electrostatic attraction between the amino groups of CH and the carboxylic–sulfate groups of anionic polymers is the main interaction leading to the formation of the PEC (7). PECs can be cross-linked by the addition of ions to form ionically cross-linked systems, for instance, calcium ions can be added to alginate (8), and pectin (9) and aluminum ions can be added to carboxymethylcellulose (4). Chitosan-based PECs are well-tolerated systems and can be used in various applications such as drug delivery systems (10).

Verapamil hydrochloride (VPL) is a freely water-soluble calcium channel blocker used in the treatment of angina pectoris, hypertension, and supraventricular tachyarrhythmias (11, 12). Upon oral administration, 90% of drug is absorbed from the gastrointestinal tract, but it has low bioavailability of 22% with a biological half-life of 4 ± 1.5 h (13).

In the present study, polyelectrolyte complex beads were prepared using CH (cationic polymer) along with three anionic polymers (sodium alginate, carboxymethylcellulose sodium, and k-carrageenan) for prolonged release of the water-soluble drug, VPL. The effect of the concentrations of CH and counter ions and the pH of the coagulation medium on the formation and performance of PEC beads was studied.

MATERIALS AND METHODS

Materials

Verapamil HCl was a kind gift sample from Unicare Pvt. Ltd. (India) and Torrent Pharmaceuticals Ltd. (India). Chitosan (minimum 80% deacetylated) was a gift sample from Mahtani Chitosan Pvt. Ltd. (India). Sodium alginate (ALG) was obtained from Snap Natural and Alginate Pvt. Ltd. (India). *k*-Carrageenan (CAR) was obtained from Sigma-Aldrich (USA). Carboxymethylcellulose sodium (CMC), calcium chloride, aluminum chloride, potassium chloride, and glacial acetic acid were obtained from SD Fine Chem Ltd. (India).

Methods

Preparation of PEC Beads

The preparation details of PEC beads are given in Table 1. PEC beads were prepared by an ionic gelation method using varied concentrations (0.5%, 1%, and 1.5% w/w) of CH along with fixed concentrations of ALG, CMC, and CAR in the presence of calcium, aluminum, and potassium as counter ions. The amount of VPL was kept constant (1% w/v). Homogeneous aqueous solutions of CH and calcium chloride/aluminum chloride/potassium chloride were

*Corresponding author.

Table 1. Formulation Details of Chitosan-Based Polyelectrolyte Complex Beads

Code	VPL (% w/v)	CH (% w/v)	ALG (%w/v)	CMC (%w/v)	CAR (% w/v)	CaCl ₂ (% w/v)	AlCl ₃ (% w/v)	KCl (% w/v)
CAC1 _a	1	0.5	3	--	--	2	--	--
CAC1 _b	1	0.5	3	--	--	2	--	--
CAC2 _a	1	1	3	--	--	2	--	--
CAC2 _b	1	1	3	--	--	2	--	--
CAC3 _a	1	1.5	3	--	--	2	--	--
CAC3 _b	1	1.5	3	--	--	2	--	--
CAA1 _a	1	0.5	3	--	--	--	2	--
CAA1 _b	1	0.5	3	--	--	--	2	--
CAA2 _a	1	1	3	--	--	--	2	--
CAA2 _b	1	1	3	--	--	--	2	--
CAA3 _a	1	1.5	3	--	--	--	2	--
CAA3 _b	1	1.5	3	--	--	--	2	--
CC1 _a	1	0.5	--	3	--	--	2	--
CC1 _b	1	0.5	--	3	--	--	2	--
CC2 _a	1	1	--	3	--	--	2	--
CC2 _b	1	1	--	3	--	--	2	--
CC3 _a	1	1.5	--	3	--	--	2	--
CC3 _b	1	1.5	--	3	--	--	2	--
CK1 _a	1	0.5	--	--	2.5	--	--	4
CK1 _b	1	0.5	--	--	2.5	--	--	4
CK2 _a	1	1	--	--	2.5	--	--	4
CK2 _b	1	1	--	--	2.5	--	--	4
CK3 _a	1	1.5	--	--	2.5	--	--	4
CK3 _b	1	1.5	--	--	2.5	--	--	4

used as coagulation media, and the pH was adjusted to 2 or 4. The CH was dissolved in acetic acid solution (1% v/v), and the pH was adjusted using 1 M HCl and 1 M NaOH. The mixtures of ALG/CMC/CAR and drug in distilled water were dropped through a 30-gauge needle into the coagulation media with appropriate mechanical stirring. The beads were then filtered, washed, and dried at room temperature for 24 h.

Scanning Electron Microscopy (SEM)

The surface morphology of the beads was examined by SEM (SEM LEO 14 SSVP, Cambridge, UK) mounted with a digital camera. All the samples were sputter-coated with gold-palladium before observation and mounted directly onto the SEM sample holder. Micrographs were obtained using an XL 30 field emission environmental microscope with acceleration voltages of 15 and 20 kv.

Differential Scanning Calorimetry (DSC)

DSC thermograms were obtained using an automatic thermal analyzer system (Perkin Elmer DSC Instrument, Japan). Temperature calibration was performed using in-

dium as the standard. Samples were crimped in a standard aluminum pan and heated from 50 to 300 °C at a heating rate of 10 °C/min under constant purging of dry nitrogen at 30 mL/min. An empty pan, sealed in the same manner as the samples, was used as a reference.

Fourier Transformation Infrared (FTIR) Spectroscopy

Drug-polymer and polymer-polymer interactions were studied by FTIR spectrometer (Perkin-Elmer Spectrum-100, Japan). A potassium bromide (KBr) disc was prepared by mixing the sample with dry KBr (2% w/w), grinding the mixture into a fine powder using an agate mortar, and then compressing it into a disc in a hydraulic press at a pressure of 10,000 psi. Each KBr disc was scanned 16 times at 2 cm⁻¹/sec at a resolution of 4 cm⁻¹/sec using cosine apodization. The characteristic peaks were recorded.

Particle Size

Particle size and mean bead diameter measurements were carried out with an optical microscope. A stage micrometer was used to calculate the calibration factor. The 10-division of the stage micrometer was matched with

the division of an ocular disc, and the calibration factor was calculated. Particle size was calculated by multiplying the number of divisions of the ocular disc that the particle occupied by the calibration factor. Fifty randomly chosen beads were taken to measure their individual sizes.

Drug Entrapment Efficiency

Accurately weighed beads equivalent to 100 mg of drug were incubated in 100 mL of pH 7.4 phosphate buffer solution for 24 h at 37 °C. After 24 h, the mixture was stirred for 5 min and filtered. After suitable dilution (10 times), drug content in the filtrate was analyzed spectrophotometrically at 278 nm (Shimadzu-1700 UV-vis spectrophotometer) against a blank. The blank solution was prepared in the same manner as above using beads without the drug. The drug entrapment efficiency was calculated using the following equation:

$$\text{Drug entrapment efficiency} = \frac{\text{Experimental drug content}}{\text{Theoretical drug content}} \times 100$$

Swelling Studies

A swelling study of the beads was performed in pH 1.2 HCl buffer solution for the initial 2 h and in pH 7.4 phosphate buffer solution for the next 6 h to simulate the gastric environment. Accurately weighed amounts of beads were immersed in the respective solutions, and at fixed time intervals (every hour), the beads were separated from the medium, immediately wiped gently with paper, and reweighed. The dynamic weight change of the beads with respect to time was calculated according to the formula

$$\text{Percent weight change} = \frac{W_s - W_i}{W_i} \times 100$$

where W_s is the weight of beads in the swollen state and W_i is the initial weight of beads.

In Vitro Dissolution Study

The in vitro release of VPL from beads was carried out for 8 h using a USP Apparatus 2 paddle type dissolution tester (Electrolab, Mumbai) containing 900 mL of dissolution medium maintained at 37 ± 0.5 °C with a stirring speed of 50 rpm. For the first 2 h, pH 1.2 HCl buffer was used as dissolution medium, then it was replaced with pH 7.4 phosphate buffer for a further 6 h. At 1-h intervals, 5 mL of solution was withdrawn and analyzed spectrophotometrically for drug content at 278 nm. The volume of the dissolution medium was adjusted to 900 mL at every sampling time by replacement with 5 mL of the same medium.

The spectrophotometric method was validated. A stock standard solution was prepared by dissolving 100-mg samples of VPL, accurately weighed, in 100 mL buffer solutions of pH 1.2 and 7.4. The stock standard solution was scanned in the UV spectrophotometer over a wavelength range of 200–300 nm. The maximum absorbance was found at 278 nm. Hence, the same wavelength was used for the determination of VPL. Aliquots of the stock standard solution were diluted 1:100 with respective buffer solutions to give stock solutions of 10 µg/mL. Serial dilutions were made to give final concentrations of 5, 10, 15, 20, 25, and 30 µg/mL. The absorbances of these solutions were measured at 278 nm against a suitable blank. The procedure was performed in triplicate to validate the calibration curve.

RESULTS AND DISCUSSION

Formation of PEC Beads

PEC beads were prepared by the interaction of positively charged CH with negatively charged ALG, CMC, and CAR, and the pH of the coagulation solution was varied between pH 2 and 4. Various counterions like Ca^{2+} , Al^{3+} , and K^+ were added to improve the mechanical strength of the beads. The electrostatic attraction between the amino ($-\text{NH}_3^+$) groups of CH and the carboxylic ($-\text{COO}^-$) groups of ALG and CMC and the sulfonic ($-\text{SO}_4^-$) groups of CAR resulted into the formation of polyelectrolyte complexes. The CH forms the outer layer of the beads, and higher concentrations of CH provide a higher charge density of amino groups. This results in higher cross-linking of PEC and thus produces a stronger PEC membrane. Only anionic polymer that did not interact completely with CH was present in the core of the beads.

Morphology of PEC Beads

The CH/ALG beads prepared using CaCl_2 were spherical with rough surfaces (Figure 1A). When AlCl_3 was used as counterion, the beads were smoother but flattened and disc-shaped with collapsed centers (Figure 1B). The CH/CMC beads prepared at pH 2 were spherical with a rough and dense surface (Figure 1C), and at pH 4, beads were flattened and disc-shaped with collapsed centers along with surface folding (Figure 1D). CH/CAR beads were spherical with smoother surfaces (Figure 1E).

Differential Scanning Calorimetry

The DSC thermograms of VPL, CH, ALG, CMC, CAR, and VPL-loaded CH/ALG, CH/CMC, and CH/CAR beads are shown in Figure 2. The thermogram of VPL exhibits a sharp endothermic peak at 146 °C. The thermograms of CH, ALG, CMC, and CAR exhibit endothermic peaks at 86, 87, 72, and 81 °C, respectively, due to evaporation of absorbed water. The thermograms of CH also show an exothermic peak at 262 °C, which indicates the onset of degradation. Whereas ALG shows two exothermic peaks at 251 °C and 265 °C, similarly CMC and CAR show exothermic peaks at 250 °C

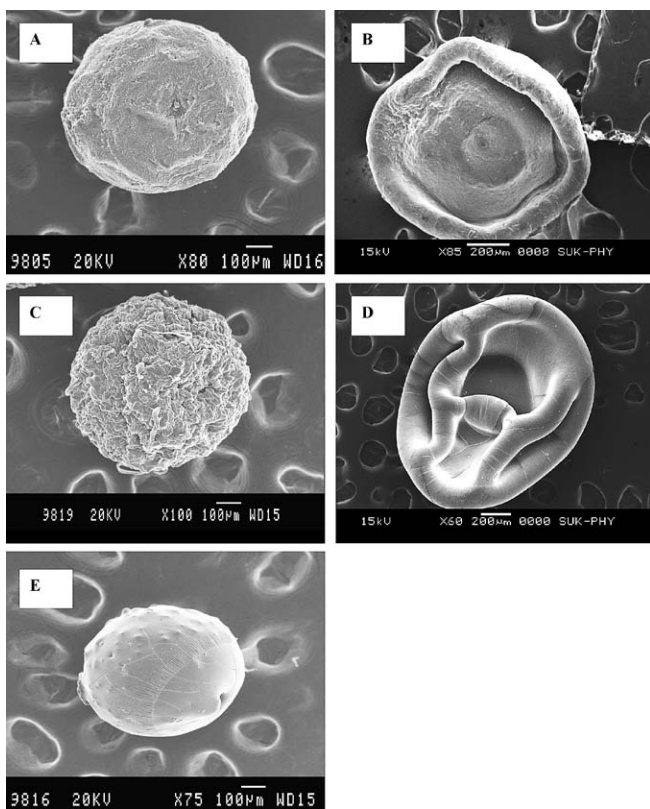


Figure 1. Scanning electron micrographs of VPL-loaded CH/ALG beads formulated with (A) CaCl_2 and (B) AlCl_3 ; CH/CMC beads formulated at coagulation medium (C) pH 2 and (D) pH 4; and (E) CH/CAR beads.

and 265 °C, respectively. In DSC thermograms of VPL-loaded CH/ALG beads, the peak corresponding to drug was shifted from 146 °C to 179 °C; the peaks corresponding to CH and ALG disappeared, and a coupled peak at 193 °C appeared. For VPL-loaded CH/CMC beads, two endothermic peaks were observed at 179 °C and 187 °C. The thermogram of VPL-loaded CH/CAR beads does not show any distinct peak but has a less intense exothermic peak at 245 °C. The results of drug-loaded beads suggest that a polyelectrolyte complex is formed between CH and ALG, CMC, and CAR during preparation. However, the disappearance or shifting of the VPL peaks indicates that most of the drug was uniformly dispersed at the molecular level in the beads or it may be caused by the electrostatic interaction between charged VPL and polymers (17).

Fourier Transformation Infrared Spectroscopy

The FTIR spectra of VPL, CH, ALG, CMC, CAR, and VPL-loaded CH/ALG, CH/CMC, and CH/CAR beads are shown in Figure 3. The FTIR spectrum of VPL exhibits a sharp characteristic absorption peak at 2236 cm^{-1} confirming the presence of $\text{C}\equiv\text{N}$ groups in the drug molecule. An absorption peak at 2837 cm^{-1} is due to C–H stretching of the VPL methoxy groups. The other characteristic peaks are in concurrence with the structure of the drug. Since the CH,

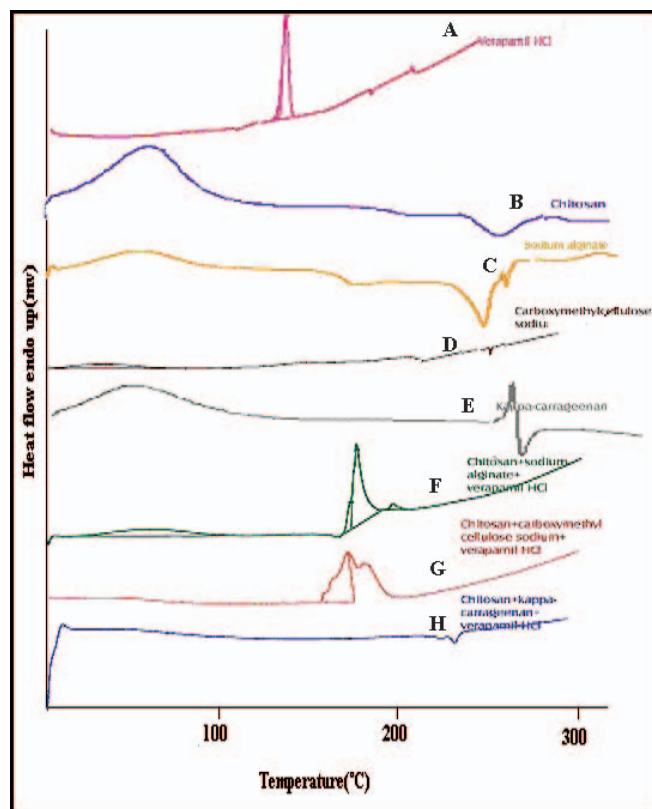


Figure 2. DSC thermograms of (A) VPL, (B) chitosan, (C) ALG, (D) CMC, (E) CAR, (F) CH/ALG beads, (G) CH/CMC beads, and (H) CH/CAR beads.

ALG, CMC, and CAR are carbohydrate polymers, they have –OH groups in their structure, which was confirmed by the broad peak between $3100\text{–}3600\text{ cm}^{-1}$. The FTIR spectrum of CH also shows a weak peak of C–H stretching at 2875 cm^{-1} and a bending vibration peak of the N–H of non-acylated 2-amino glucose primary amines at 1534 cm^{-1} . The FTIR spectra of ALG and CMC show broad peaks near 1700 cm^{-1} , confirming the presence of a –COO^- group in their structures. The spectrum of CAR shows a broad absorption peak around 1350 cm^{-1} , which is due to sulphonic acid (–SO_4^-) groups. In the FTIR spectrum of VPL-loaded CH/ALG beads, the peak at 1700 cm^{-1} (which was observed in ALG spectra) is coupled to form a broad peak near $2200\text{–}2400\text{ cm}^{-1}$. In the FTIR spectrum of VPL-loaded CH/CMC beads, the peak observed at 1200 cm^{-1} in CMC is shifted to $750\text{–}800\text{ cm}^{-1}$. In the spectrum of CH/CAR beads, the peak at 2200 cm^{-1} , which was observed in CAR spectrum, disappeared. It also shows an absorption peak around $1600\text{–}1700\text{ cm}^{-1}$, which is not observed in the spectrum of CH and CAR. This is evidence for the formation of polyelectrolyte complexes between CH and ALG, CMC, and CAR during preparation. However, the characteristic peaks of VPL have changed or shifted in the spectra of the formulations. In the spectrum of VPL-loaded CH/ALG beads, the broad peak around 2500 cm^{-1} is not observed along with sharp peaks at 2300 cm^{-1} and $1600\text{–}1700\text{ cm}^{-1}$. These peaks are absent in spectrum of

VPL. Similarly, in the spectrum of CH/CAR beads, two broad peaks are observed at 2900 cm^{-1} and 2500 cm^{-1} . These peaks are absent in the spectrum of VPL. This might be due to the electrostatic interaction of VPL with ALG, CMC, and CAR during the formation of PECs.

Size of the Beads

The size of the beads is summarized in Table 2. Bead size was influenced by the concentrations of CH and counterions and the pH of coagulation medium. The orifice of the needle and the rate of pouring the polymeric solution into the counter ion solution were fixed. The mean particle size of CH/ALG beads prepared with CaCl_2 was between 556 and $739\text{ }\mu\text{m}$, whereas formulations containing AlCl_3 were in the range of 705 – $865\text{ }\mu\text{m}$. The particle size range for CH/CMC beads was 698 – $896\text{ }\mu\text{m}$ and for CH/CAR beads it was 683 – $889\text{ }\mu\text{m}$. All preparations showed an increase in size as the concentration of CH increased, which was due to extra coating of CH with increasing concentration (12). The change in pH of counter ion medium did not show any significant increase in the particle size.

Table 2. Evaluation Parameters of PEC Beads

Code	Particle size (μm) (mean \pm SD)	Percent drug entrapment (mean \pm SD)
CAC1 _a	570.24 \pm 66.56	91.22 \pm 1.05
CAC1 _b	556.26 \pm 96.00	93.58 \pm 0.82
CAC2 _a	704.64 \pm 77.07	94.14 \pm 1.33
CAC2 _b	701.24 \pm 78.48	94.85 \pm 1.56
CAC3 _a	729.86 \pm 80.97	96.46 \pm 0.60
CAC3 _b	739.80 \pm 89.19	97.08 \pm 0.73
CAA1 _a	705.76 \pm 69.56	91.07 \pm 1.52
CAA1 _b	706.32 \pm 70.02	93.21 \pm 1.25
CAA2 _a	813.30 \pm 52.32	91.90 \pm 0.78
CAA2 _b	819.60 \pm 59.13	94.04 \pm 1.55
CAA3 _a	870.64 \pm 66.46	94.71 \pm 1.40
CAA3 _b	865.72 \pm 84.45	95.80 \pm 0.73
CC1 _a	698.54 \pm 57.67	86.97 \pm 1.90
CC1 _b	700.26 \pm 66.52	87.16 \pm 0.76
CC2 _a	820.26 \pm 52.27	91.23 \pm 0.35
CC2 _b	835.80 \pm 54.07	91.59 \pm 1.15
CC3 _a	867.76 \pm 55.62	93.24 \pm 2.45
CC3 _b	896.18 \pm 53.98	96.14 \pm 1.79
CK1 _a	704.92 \pm 67.95	80.01 \pm 0.59
CK1 _b	683.74 \pm 30.34	86.30 \pm 1.65
CK2 _a	769.10 \pm 51.40	87.69 \pm 1.04
CK2 _b	781.58 \pm 82.62	88.20 \pm 1.46
CK3 _a	871.42 \pm 69.26	89.87 \pm 1.59
CK3 _b	889.94 \pm 71.61	90.98 \pm 1.63

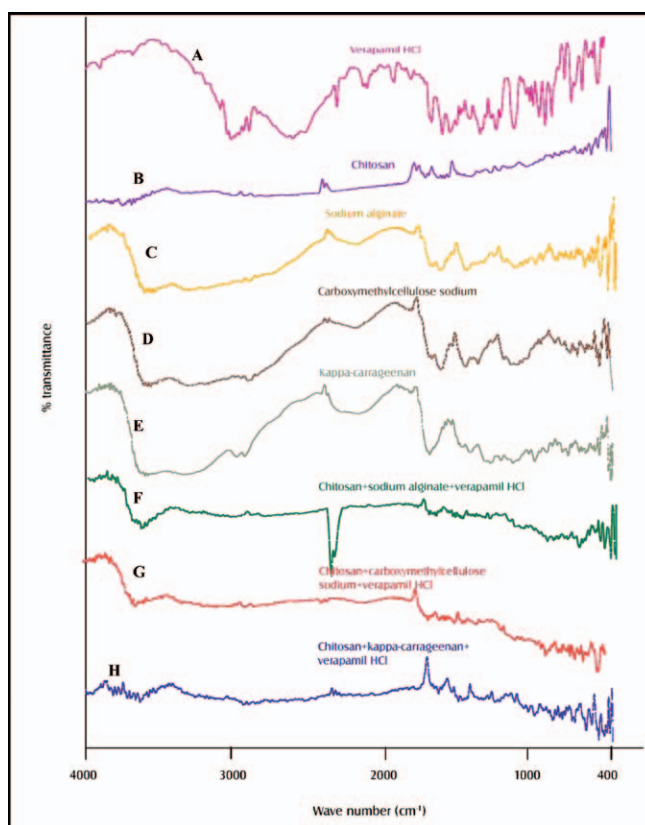


Figure 3. FTIR spectra of (A) VPL, (B) chitosan, (C) ALG, (D) CMC, (E) CAR, (F) CH/ALG beads, (G) CH/CMC beads, and (H) CH/CAR beads.

Drug Entrapment Efficiency

The results of entrapment efficiency are presented in Table 2. The prepared PEC beads showed high entrapment efficiency in the range of 80.01 – 97.08% , suggesting that the ionic gelation method was effective for the entrapment of VPL. The concentration of CH and the pH of the coagulation medium had an effect on the entrapment of VPL. With an increase in CH concentration and a change in the pH of coagulation medium, there was an increase in the entrapment efficiency of VPL. At higher concentrations of polymer and pH values corresponding to their ionized states, there will be an increase in both the charge density of the polymers, which leads to higher cross-linking, and ionic interaction. As a result, less drug was lost from the PEC beads during gelation, and hence a higher percent entrapment occurred (11, 12). The beads prepared with CAR showed less entrapment efficiency as compared with ALG and CMC because there was less cross-linking with low ionic interaction resulting in an increase in drug loss during the gelation process.

Swelling Studies

The swelling was measured by incubation and mass measurement method. The prepared PEC beads showed pH-sensitive swelling behavior (Figure 4). The degree

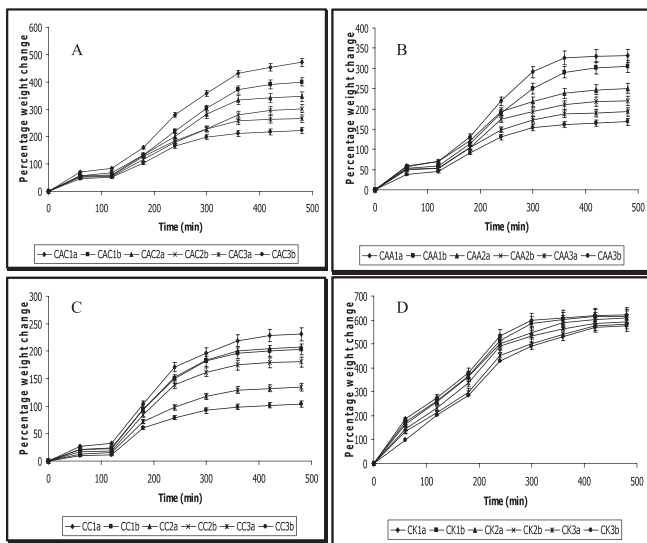


Figure 4. Swelling behavior of CH/ALG beads formulated with (A) CaCl_2 , (B) AlCl_3 , (C) CH/CMC beads, and (D) CH/CAR beads.

of swelling was mainly affected by pH of the dissolution medium, type of anionic polymer, counterion, pH of counter ion medium, and concentration of CH. All the beads show low swelling in pH 1.2 HCl buffer, and after incubating the same beads in pH 7.4 phosphate buffer, the degree of swelling increased. At pH 1.2, the amino ($-\text{NH}_3^+$) groups of chitosan were protonated, thereby increasing charge density, which interacts strongly with the carboxylic (COO^-) groups of ALG, CMC, and sulphonic groups ($-\text{SO}_4^-$) of CAR. This leads to the formation of stronger polyelectrolyte complexes, and hence the degree of swelling is reduced. At pH 7.4, the deprotonation of chitosan weakens the extent of ionic interactions, which leads to complex dissociation, and hence the degree of swelling is increased (11). The degree of swelling in CH/ALG beads was affected by counter ions (Figures 4A,B). The swelling of the beads prepared with CaCl_2 was greater than that for beads prepared with AlCl_3 , which may be because the trivalent ions (Al^{3+}) increase the protonation of the carboxylic (COO^-) groups and form a denser network. In addition, disc-shaped particles were formed, which restricts the entry of dissolution fluids into the beads. The degree of swelling in CH/CMC beads was much less (Figure 4C), indicating that strong ionic interaction occurred in the presence of AlCl_3 , which restricts the entry of dissolution fluids. The degree of swelling of CH/CAR beads was greater (Figure 4D) due to rapid dissociation of PEC in acidic as well as in alkaline pH because of weak ionic interactions. As the concentration of chitosan increased, the degree of swelling decreased due to decreased solubility of chitosan in pH 7.4 dissolution medium (13). When the pH of the counterion medium was changed from pH 2 to 4, the degree of swelling decreased due to increased protonation of the

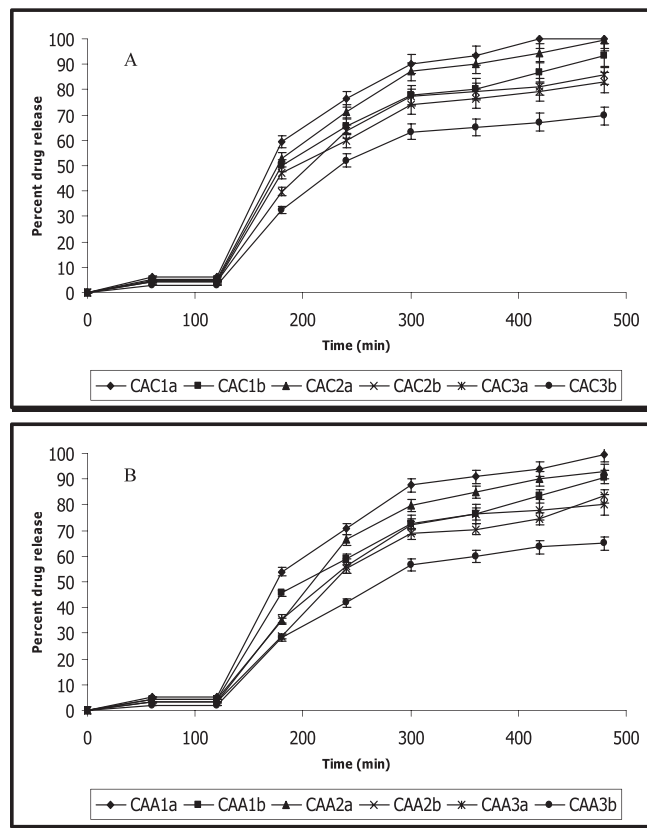


Figure 5. In vitro dissolution profiles of CH/ALG beads formulated with (A) CaCl_2 and (B) AlCl_3 .

amino $-\text{NH}_3^+$ groups present, resulting in higher cross-linking of PEC and thus a stronger PEC membrane.

In Vitro Dissolution Study

The in vitro dissolution data for CH/ALG, CH/CMC, and CH/CAR are presented in Figures 5 and 6. The release of VPL from PEC beads was mainly affected by the dissolution medium, concentration of chitosan, type of anionic polymers used, pH of the coagulation medium, and counterion. The release of VPL was very slow in pH 1.2 HCl buffer. After 2 h, approximately 6.19%, 1.29%, and 14.07 % of drug was released from CH/ALG, CH/CMC, and CH/CAR beads, respectively. At the acidic pH of the dissolution medium, the charge density of chitosan was sufficiently high, and the ionic interaction increased resulting in the formation of a much stronger network. In the second phase of the study using pH 7.4 phosphate buffer, the release was rapid, and a maximum of 93.53%, 80.35%, and 97.46 % of drug was released from CH/ALG, CH/CMC, and CH/CAR beads, respectively, within 6 h. The ionic interactions between chitosan and negatively charged polymers might have been reduced at pH 7.4, forming a loose network with increased porous surface. This allows a large amount of dissolution medium along with counterions to enter into the PEC matrix.

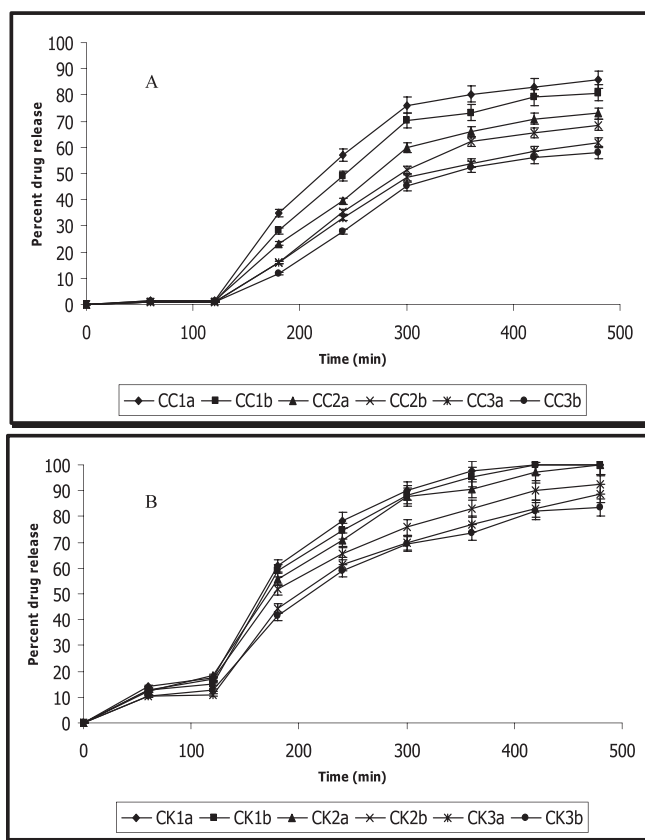


Figure 6. In vitro dissolution profiles of (A) CH/CMC beads and (B) CH/CAR beads.

Hence, in pH 7.4 phosphate buffer, rapid dissociation of the PEC membrane may occur leading to drug release with a burst effect (11). The CH/CMC PEC beads showed sustained release of VPL (Figure 6A) due to formation of a stronger PEC membrane that restricts the easy entry of dissolution medium into the PEC matrix. The release of VPL from CH/CAR beads was very rapid (Figure 6B), because of the formation of a loose network of PEC which dissociates and disintegrates rapidly in phosphate buffer. With an increase in CH concentration, the interaction between the two polymers increased with the formation of a closer network, which showed a decrease in the diffusion of drug from the beads (14). When the pH of the coagulation medium was changed from pH 2 to 4, the charge density of the polymers increased. This resulted in more ionic interactions and the formation of a strong PEC membrane that did not swell or burst easily, thereby sustaining the release of VPL. The release data were subjected to the zero-order, first-order, Higuchi, Korsmeyer–Peppas, erosion, and Baker–Lonsdale models to establish the release mechanism and kinetics of drug release from PEC beads (Table 3). It was suggested that drug release followed first-order kinetics, and drug diffused out by erosion of the surface through dissociation of the PEC membrane. We have determined the release mechanism using the Korsmeyer–Peppas model. According to this model, n values indicate the type of release mechanism. For spheres, values of n between 0.45 and 0.85 are an indication of both diffusion-controlled and swelling-controlled release mechanisms (anomalous transport). Values greater than 0.85 and 1.0 indicate Case II and Super Case II transports, respectively, which relate to polymer relaxation. Because the values of n obtained

Table 3. Regression Analysis and Correlation Coefficient Values According to Various Release Kinetics Models

Code	Zero order		First order		Higuchi		Korsmeyer-Peppas			Erosion		Baker-Lonsdale	
	r	SSR	r	SSR	r	SSR	r	SSR	n	r	SSR	r	SSR
CAC1 _a	0.939	1770.20	-0.962	0.108	0.920	2293.70	0.910	0.342	1.587	-0.970	0.073	0.970	0.515
CAC2 _a	0.947	1438.70	-0.938	0.518	0.921	2141.60	0.914	0.364	1.678	-0.981	0.027	0.971	0.418
CAC3 _a	0.944	1143.20	-0.972	0.051	0.916	1747.50	0.919	0.359	1.723	-0.966	0.021	0.957	0.399
CAA1 _a	0.946	1470.70	-0.932	0.588	0.920	2149.50	0.913	0.363	1.668	-0.980	0.029	0.970	0.435
CAA2 _a	0.956	1094.20	-0.978	0.070	0.915	2087.00	0.929	0.328	1.775	-0.977	0.021	0.969	0.375
CAA3 _a	0.950	958.35	0.969	0.044	0.914	1620.90	0.920	0.416	1.871	-0.964	0.018	0.958	0.337
CC1 _a	0.953	1054.80	-0.972	0.055	0.908	1995.10	0.913	0.749	2.400	-0.969	0.020	0.962	0.371
CC2 _a	0.968	501.25	0.973	0.024	0.906	1406.00	0.932	0.490	2.220	-0.973	0.010	0.971	0.176
CC3 _a	0.969	339.98	-0.973	0.013	0.902	1034.80	0.933	0.555	2.398	-0.973	0.006	0.971	0.113
CK1 _a	0.947	1369.70	-0.959	0.215	0.944	1452.30	0.942	0.097	1.087	-0.980	0.049	0.976	0.391
CK2 _a	0.963	910.92	-0.967	0.137	0.951	1201.80	0.962	0.067	1.122	-0.974	0.046	0.986	0.203
CK3 _a	0.969	579.23	-0.987	0.024	0.944	1031.80	0.940	0.122	1.187	-0.988	0.007	0.981	0.159

r : regression coefficient
SSR: sum of squares of residual
 n : slope

for all the formulations are greater than 1.0, the release mechanism is Super Case-II transport.

CONCLUSIONS

PEC beads were successfully prepared by an ionic gelation method using positively charged chitosan and negatively charged sodium alginate, carboxymethylcellulose sodium, and k-carrageenan for the prolonged release of the water-soluble drug, VPL. The SEM study confirmed the shape of the beads that were prepared by changing the counterion and pH of the coagulation medium. The particle size range was 556–896 μm , and drug entrapment efficiency was as high as 97%. The beads showed pH-sensitive swelling with lower swelling in pH 1.2 hydrochloric acid buffer and higher swelling in pH 7.4 phosphate buffer. The in vitro release of VPL was very slow in hydrochloric acid buffer as compared with phosphate buffer. Among the anionic polymers used, carboxymethylcellulose sodium showed prolonged release of drug more efficiently. Hence, this study indicates that the proper selection of reaction pH, counter ions, and concentration of chitosan can result in the formation of stable PEC beads for the prolonged release of highly water-soluble drugs.

ACKNOWLEDGMENTS

The authors are thankful to the Principal and Management of Luqman College of Pharmacy, Gulbarga (India), for providing all the necessary facilities to carry out this research.

REFERENCES

1. Bhattarai, N.; Gunn, J. J.; Zhang, M. Chitosan-based hydrogels for controlled, localized drug delivery. *Adv. Drug Deliv. Rev.* **2010**, *62* (1), 83–99.
2. Naidu, V. G. M.; Madhusudhana, K.; Sashidhar, R. B.; Ramakrishna, S.; Khar, R. K.; Ahmed, F. J.; Diwan, P. V. Polyelectrolyte complexes of gum kondagogu and chitosan, as diclofenac carriers. *Carbohydr. Polym.* **2009**, *76* (3), 464–471.
3. Felt, O.; Buri, P.; Gurny, R. Chitosan: A Unique Polysaccharide for Drug Delivery. *Drug Dev. Ind. Pharm.* **1998**, *24* (11), 979–993.
4. Lankalapalli, L.; Kolapalli, V. R. M. Polyelectrolyte Complexes: A Review of their Applicability in Drug Delivery Technology. *Indian J. Pharm. Sci.* **2009**, *71* (5), 481–487.
5. Berger, J.; Reist, M.; Mayer, J. M.; Felt, O.; Peppas, N. A.; Gurny, R. Structure and interactions in covalently and ionically crosslinked chitosan hydrogels for biomedical applications. *Eur. J. Pharm. Biopharm.* **2004**, *57* (1), 19–34.
6. Long, D. D.; VanLuyen, D. Chitosan–Carboxymethylcellulose Hydrogels as Supports for Cell Immobilization. *J. Macromol. Sci. A* **1996**, *33* (12), 1875–1884.
7. Wang, H.; Li, W.; Lu, Y.; Wang, Z. Studies on chitosan and poly(acrylic acid) Interpolymer Complex I. Preparation, structure, pH-sensitivity, and salt sensitivity of complex-forming poly(acrylic acid): Chitosan semi-interpenetrating polymer network. *J. Appl. Polym. Sci.* **1997**, *65* (8), 1445–1450.
8. Takahashi, T.; Takayama, K.; Machida, Y.; Nagai, T. Characteristics of Polyion Complexes of Chitosan with Sodium Alginate and Sodium Polyacrylate. *Int. J. Pharm.* **1990**, *61* (1–2), 35–41.
9. Lee, J. W.; Kim, S. Y.; Kim, S. S.; Lee, Y. M.; Lee, K. H.; Kim, S. J. Synthesis and Characteristics of Interpenetrating Polymer Network Hydrogel Composed of Chitosan and Poly(acrylic acid). *J. Appl. Polym. Sci.* **1999**, *73* (1), 113–120.
10. Hamman, J. H. Chitosan Based Polyelectrolyte Complexes as Potential Carrier Materials in Drug Delivery Systems. *Mar. Drugs* **2010**, *8* (4), 1305–1322.
11. Patel, A.; Moin, M.; Shah, D.; Patel, V. Development and In Vivo Floating Behavior of Verapamil HCl Intra-gastric Floating Tablets. *AAPS PharmSciTech* **2009**, *10* (1), 310–315.
12. Kunte, S.; Tandale, P. Fast dissolving strips: A novel approach for the delivery of verapamil. *J. Pharm. Bioallied Sci.* **2010**, *2* (4), 325–328.
13. Chandira, M.; Debjit, M.; Chiranjib, K.; Jayakar, B. Formulation, design and development of buccoadhesive tablets of verapamil hydrochloride. *Int. J. PharmTech Res.* **2009**, *1* (4), 1663–1677.
14. Daly, M. M.; Knorr, D. Chitosan-Alginate Complex Coacervate Capsules: Effects of Calcium Chloride, Plasticizers, and Polyelectrolytes on Mechanical Stability. *Biotechnol. Prog.* **1988**, *4* (2), 76–81.